Plume Plasma Measurements of a 20-cm Xenon Ion Thruster Using a Multiple-Probe Array

IEPC-2015-222／ISTS-2015-b-222

Presented at Joint Conference of 30th International Symposium on Space Technology and Science
34th International Electric Propulsion Conference and 6th Nano-satellite Symposium,
Hyogo-Kobe, Japan
July 4 – 10, 2015

Zun Zhang[1], Haibin Tang[2],
Beihang University, Beijing, 100191, China

Jue Wang[3], Min Wang [4], and Zheng Wen[5]
Institute of Telecommunication Satellite CAST, Beijing, 100094, China

Abstract: A multiple-probe array was designed and implemented on a laboratory model 20-cm ion thruster in order to examine the plasma plume properties thoroughly, which could be vital to fully understand the plume plasma interactions with spacecrafts and validate the ongoing modeling efforts. The probe array includes a retarding potential analyzer (RPA), a Faraday probe, an Emissive probe, a flat single Langmuir probe and a triple Langmuir probe. RPA test results show that the ion energy within the beam plasma is about 1000 eV and remains nearly constant along the increased axial distances, whereas the ion energy decreases by 7% from the centerline to 200 mm off centerline at an axial position of 500 mm. In addition, Faraday probe measurements provide a 2-D current density contour map, which shows that the maximum current density occurs at the centerline near the thruster, whereas the minimum current density occurs at the wings. The current density decreases with both increased radial and axial distances and larger current density gradient is along the radial direction. Moreover, the plasma potential determined from the emissive probe by a cross point technique is 18 V, and the electron temperature and density derived from both the triple and single Langmuir probe lies in the range of 1-4 eV, 0.4-2×10^{15} m^{-3}, respectively.

Nomenclature

A	=	probe area
e	=	electron charge, 1.6×10^{-19} C
k	=	Boltzmann constant, 1.38×10^{-23} J/K
I_{sat}	=	ion saturation current
I_{Bohm}	=	Bohm current
j	=	Current density
R	=	shunt resistance
m_i	=	ion mass
n_e	=	electron density
T_e	=	electron temperature

[1] PhD Student, School of Astronautics, and zhangzun@buaa.edu.cn.
[2] Professor, School of Astronautics, and thb@buaa.edu.cn.
[3] Doctor, Institute of Telecommunication Satellite, and charlyjw2001@163.com.
[4] Senior Engineer, Institute of Telecommunication Satellite, and charlyjw2001@163.com.
[5] Doctor, Institute of Telecommunication Satellite, and 13701247765@139.com.

V = voltage differences on the shunt resistance
V_p = probe voltage
V_{d2} = measured voltage difference between the positive probe and the floating probe
V_{d3} = fixed voltage between the positive and negative probes
V_f = floating potential
V_s = plasma potential

I. Introduction

AN ion thruster is a type of electrostatic propulsion system in which the effective exhaust velocity is not limited by the energy released from chemical propellants. In the ion thruster, the propellant is ionized into plasma by the electrical power, and the ions from the plasma are accelerated by the electrical power unit to produce the thrust. The required electrical power can be obtained from solar, nuclear, and other forms of energy. This means that to achieve a given amount of thrust, the required propellant quantity could be relatively small, which can be translated into an extended lifetime, a larger payload, a lower cost, or a combination of these factors.[1,2] Based on their advantages of high-efficiency, high-specific-impulse, and long-lifetime, ion thrusters are popularly used in spacecraft propulsion system designs, such as the 30-cm NASA Solar Electric Propulsion Technology Applications Readiness (NSTAR) ion engine,[3] UK-S series of Kaufman type ion thrusters,[4] the Ion Engine Subsystem (IES) of Engineering Test Satellite 8 (ETS-8), and the 20-cm ion thruster on ShiJian Satellite (SJ-9A).[5]

Although ion thrusters offer many advantages, several problems need to be addressed in order to successfully implement ion thrusters on board spacecrafts. One of these problems regards the ion thruster plume interactions with spacecrafts.[6,7] Ion thruster plumes primarily consist of electrons, high energy beam ions, and low energy charge exchange ions. These particles could interact with and even damage the sensitive surfaces of the spacecraft. For example, high energy ions can impact the surface of the spacecraft resulting in material erosion. In turn, this sputtered material can contaminate solar arrays and other sensitive surfaces. Also, low energy charge exchange ions could flow back to the spacecraft and alter its potential. Plume impingement on solar arrays can result in thrust loss and torque perturbation, causing a change in spacecraft attitude. In addition, plume optical emission can interfere with sensitive optical instruments and the plume electromagnetic field can lead to distortion of communication signals. Therefore, the plume plasma parameters of ion thrusters are vital to the thruster designs and the successful combination between ion thrusters and onboard spacecrafts.

Numerous studies have been conducted to determine the distribution information of the plasma parameters of ion thrusters, which contributed a lot to the development of ion thrusters.[8] As early as 1965, Sellen, et al.[9] tested a cesium ion source with the Faraday probe, single Langmuir probe, and emissive probe to obtain the current density, electron temperature, and plasma potential profiles at various axial and radial positions respectively. Coben[10] performed the Faraday and single Langmuir probe experiments on a 10-cm-diameter ion thruster to study the diffusion process of the ion thruster. Komatsu, et al.[11] applied a Faraday probe to test a 30 cm mercury ion thruster in 1975. Because of the absence of Langmuir probe tests they calculated electron temperatures from the floating potentials which were derived from Faraday probe results. Komatsu, et al.[12] using a retarding potential analyzer (RPA) with different grid designs to study the distribution of ion populations with different energies. De Boer, et al. (1996)[1,13] applied both the single and double Langmuir probe to investigate the plume plasma properties of a 10-cm ion thruster, and they obtained the distribution profiles of electron temperature, ion density, and plasma potential. At the same year, Keefer and Semak[14] also applied a single Langmuir probe to study the radial and axial distributions of an ion thruster's plasma parameters. They concluded a significantly lower experimental value of electron temperature than previously reported. J. Wang, et al.[15] did in situ measurements of the 30 cm-Xe ion thruster used in the Deep Space One (DS1) spacecraft in 2000. The RPA and single Langmuir probe are used to obtain the ion energy, electron temperature and density profiles with the ion thruster worked at three different thrust levels. In 2001, Ozaki, et al.[16] tested the ETS-8 ion thruster with a single Langmuir probe and delivered the electron temperature results. In 2011, Yamamoto, et al.[17] applied a non-intrusive laser based optical method called Laser Thomson scattering (LTS) technique to examine the plasma number density and electron temperature properties of a miniature xenon ion thruster. From these valuable researches described above, several different kinds of diagnostics have been developed to obtain the plasma properties. These diagnostics include the retarding potential analyzer (RPA), Faraday probe, emissive probe, Langmuir probe, laser Thomson scattering method and so on.

A laboratory model 20-cm ion thruster similar to the ion thruster employed for SJ-9A Satellite was tested with the collaboration between Beihang University and Institute of Telecommunication Satellite CAST. We designed and applied a multiple-probe array which consists of a RPA, a Faraday probe, an emissive probe, a flat single Langmuir probe and a triple Langmuir probe in order to obtain the spatial distribution of the ion energy, current density, plasma potential, electron temperature and density. These plasma parameters will play an important role in the validation of numerical models and optimization of thruster designs.

The paper is organized as follows: The experimental apparatus including the ion thruster, vacuum chamber, and multiple probes are presented in Sec. II. The obtained profiles of the ion energy, current density, plasma potential, electron temperature, and electron density are shown and discussed in Sec.III. The conclusions are summarized in Sec. IV.

II. Experimental Apparatus

A. Ion thruster

The ion thruster applied in this study is a 20-cm-diameter Kaufman ion thruster, which is a laboratory model similar to the ion thruster employed for the SJ-9A Satellite launched in October, 2012. [18,19] This thruster uses xenon as propellant and has twin grids that are convex outward. The thruster can provide a thrust of 40±2 mN under a beam current of 800 mA, a beam voltage of 1080 V, a cathode current of 720 mA, a cathode voltage of 14.5 V, an anode current of 390 mA, an anode voltage of 34.5 V, a neutralizer current of 1570 mA, a neutralizer voltage of 19.5 V, an accelerator grid voltage of -190 V, a cathode xenon flow rate of 1.51 SCCM, an anode xenon flow rate of 14.4 SCCM, and a neutralizer xenon flow rate of 1.77 SCCM.

B. Vacuum Chamber

The vacuum chamber used is 5.5 m in diameter and 12.8 m in length, which is pumped by two dry vacuum pumps, two roots pumps, two molecular pumps, and two cryopumps. The characteristics of the four types of vacuum pumps are listed in Table 1. The neutral background pressure was monitored by two ionization gauges and maintained at 1.5×10^{-3} Pa during the whole experimental process.

Table 1. Characteristics of the vacuum pumps

Name	Model	Pumping speed, liters/s
dry vacuum pump	SP630	175
roots pump	WSU2001-FC	940
molecular pump	TW1600-250ISOF	1600
Cryopump	Coolvac 60000BL-LN	60000（N_2）

C. Probes

The multiple-probe array consists of a RPA, a Faraday probe, an emissive probe, a flat single Langmuir probe and a triple Langmuir probe, as shown in Fig. 1.

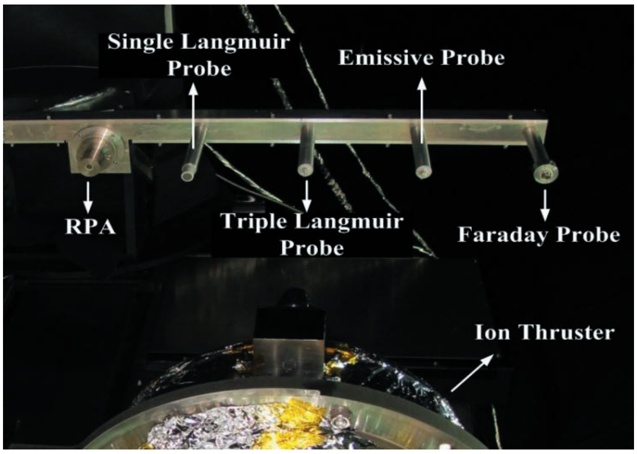

Figure 1. Multiple-probe array and the ion thruster.

1. Retarding potential analyzer

The retarding potential analyzer (RPA) is a diagnostic instrument that measures the ion energy distribution. [20,21] It consists of a current collector shielded from the plasma by a series of biased grids. Typically, four grids are used in RPAs, of which the first grid is floated to reduce plasma perturbation, the second grid is negatively biased to repel electrons, the third grid is positively biased to repel the selected ions, and the fourth grid is negatively biased to repel secondary electrons. The RPA allows only ions with energy higher than the retarding potential to reach the collector.

Our RPA design consists of only three grids without the fourth grid considering the secondary electron emission could be neglectable. The first grid is floating, and the second grid is biased to be -30V to repel electrons. Due to the possible high ion energy corresponding to the beam voltage of 1080 V, the third grid is biased a scan voltage of 0-1200 V to repel the high energy ions. The grids have an open area of 73.6% with a mesh diameter of 0.3 mm.

2. Faraday probe

The Faraday probe is a diagnostic instrument that measures current density. [22,23] Usually, it consists of a flat collector enclosed in a guard ring. Both the collector and the guard ring are biased at the same negative potentials to repel electrons. But only the current through the collector is measured to offer the current density and plume divergence information. The guard ring is used to shield the collector from low energy ions arriving from outside the collector's line of site. The separation between the collector and the guard ring must be carefully designed to ensure the sheath of the two walls could cover the gap.

The current densities are determined by Eq. (1).

$$j = \frac{V}{RA} \tag{1}$$

The Faraday probe used here is a guard ring type. The collector's diameter is 4 mm, and the minimum separation between the collector and guard ring is 1 mm. A bias voltage of -30V was supplied to the probe during the operation.

3. Emissive probe

While the single Langmuir probe offers the ability to measure several important plasma properties, its ability to determine the plasma potential accurately could be reduced substantially by non-ideal conditions such as increased sheath, strong magnetic fields and so on. Under these non-ideal conditions, the plasma potential is hard to be identified. The emissive probe could provide a highly accurate measurement of the local plasma potential by a much clear inflexion point due to the hot electron emission. Except for a provided heating current, the emissive probe is operated like a single Langmuir probe: the probe is biased to a range of voltages and the resulting current to the probe is monitored. The measurements of the biased voltage and the corresponding loop current are plotted to be the I-V characteristics, by which the plasma potential is determined.[24]

There are several techniques to determine the plasma potential such as the separation point, inflection point, floating potential inference, inflection point in the limit of zero emission methods and so on.[25]

In this study the emitting portion of the emissive probe consists of 0.1 mm diameter tungsten wire bent to form a closed loop roughly 3 mm in diameter.

4. Triple Langmuir probe

Chen and Sekiguchi [26] introduced us the triple Langmuir probe method in the year of 1965 to derive the instantaneous electron temperature and density of the plasma. Unlike the single and double Langmuir probes, triple Langmuir probe does not require the voltage sweep to determine T_e and n_i. This feature enables us to determine the instantaneous time histories of T_e and n_i within a very short time (≦1 μs). Therefore, triple Langmuir probe method could be a useful diagnostics not only for stationary plasmas but also for rapidly varying plasmas. [27,28]

The triple Langmuir probe consists of three single Langmuir probes, which are separated from each other by a certain distance. A fixed voltage V_{d3} is applied between two of those wires, and the other one is floating. The measurements of the voltage difference V_{d2} between the positive and floating wires and the loop current I_3 between the positive and negative wires were used to calculate the electron temperature and density by Eqs. (2) and (3), respectively.

$$\frac{1}{2} = \frac{1-\exp(-\frac{eV_{d2}}{kT_e})}{1-\exp(-\frac{eV_{d3}}{kT_e})} \tag{2}$$

$$n_e = \frac{I_{sat}\sqrt{m_i}\,\exp(0.5)}{Ae\sqrt{kT_e}\left[\exp\left(\frac{eV_{d2}}{kT_e}\right)-1\right]} \tag{3}$$

The triple Langmuir probe used consists of three tungsten wires, and each of them is 0.3 mm in diameter and possesses a 6.4 mm long exposed tip as the collecting conductor. These wires are configured in a regular triangle fashion, with their axis aligned with the thruster centerline. The intervals among these wires are 2 mm, which ensure that the probes do not disturb each other because the sheath around the probe is quite thin (~0.2 mm) compared with the intervals.

5. Single Langmuir probe

The single Langmuir probe method is believed to be a fundamental diagnostics to obtain plasma properties in different plasma conditions. [29,30,31] The probe I-V characteristic is created by plotting the measured current versus the applied voltage, from which the floating potential V_f is determined by finding out the voltage where the net current is zero, and the plasma potential V_s is determined by finding out the voltage where a cross point of the linear fits of the transition and electron saturation regions exists. The transition region of the I-V characteristic should be a straight line when the probe current is plotted semi-logarithmically versus the probe voltage V_p under the assumption that the electrons being measured follow the Maxwellian distribution. The inverse slope of this linear segment of the *ln*(I)-V characteristic is the value of electron temperature in eV, as shown in Eq. (4). The ion number density was calculated by Eq. (5).

$$\frac{1}{T_{ev}} = \frac{\ln(I_{total})}{V_p} \tag{4}$$

$$I_{sat} = I_{\mathrm{Bohm}} = \alpha n_e e A \sqrt{\frac{kT_e}{m_i}} \tag{5}$$

The single Langmuir probe used here is a flat type, which has a diameter of 12 mm. The probe tip is made of tungsten in order to reduce the thermal load and second electron emission.

D. Data acquisition

Probe positioning was achieved by a two-axis translation mechanism powered by two step-motors separately, which consists of two movement stand inside the vacuum chamber, and a servo control windows outside the vacuum chamber. Movement of up to 1000 mm is possible with each movement stand.

A data acquisition system with 16 isolated channels is used in the experiment to collect the simultaneous applied voltage and the corresponding probe current of all these kinds of probes. The sampling rate of the signals is 1 kHz.

III. Results and Discussion

A. Retarding potential analyzer

Figure 2 shows the original probe voltage and current of the RPA, which is combined with much high frequency noise. So the Savitzky-Golay smoothing method was used to get a smoothed I-V characteristics. The smoothed

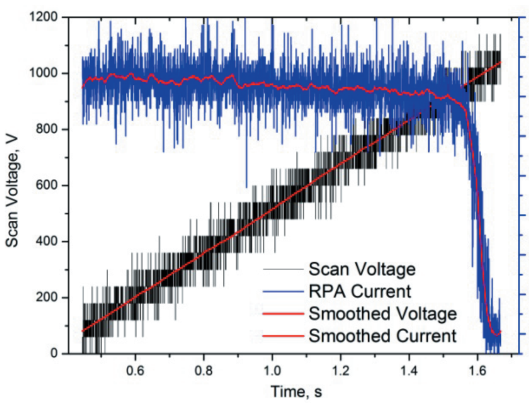

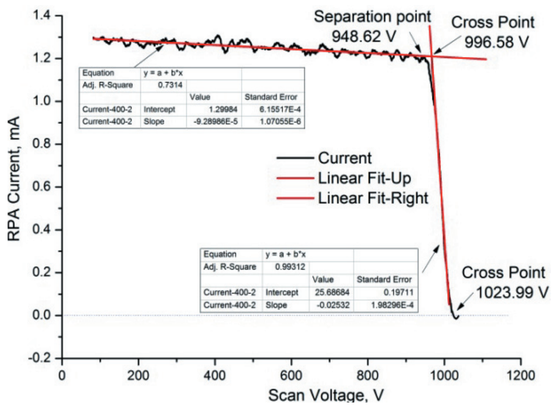

Figure 2. Original probe voltage and current of the RPA. Figure 3. Determination of the ion energy from I-V curve.

signals, which are red and centered, are also shown in Fig. 2. Due to the low ratio of the signal to noise, the differential I-V characteristics are difficult to understand. Therefore, we identified three key points to determine the ion energy distribution, as show in Fig. 3. The first point is the separation point from the up linear fit of the I-V curve, which determines the minimum energy of ions to get through the retarding potential well. The second point is the maximum ion energy, where the probe net current is zero. And the third point is the cross points of the up and right linear fits of the I-V curve, which determines the average ion energy.

RPA radial scan measurements were performed from the thruster centerline to 200 mm off centerline in a 50 mm step at an axial position of 500 mm downstream from the grid surface of the thruster. RPA I-V curves at different radius are show in Fig. 4. And the radial ion energy distribution is plotted in Fig. 5, which is determined by the three energy points described in the above paragraph. We can see from Fig. 5 that the ion energy decrease a little (~7%) from the centerline to 200 mm off centerline.

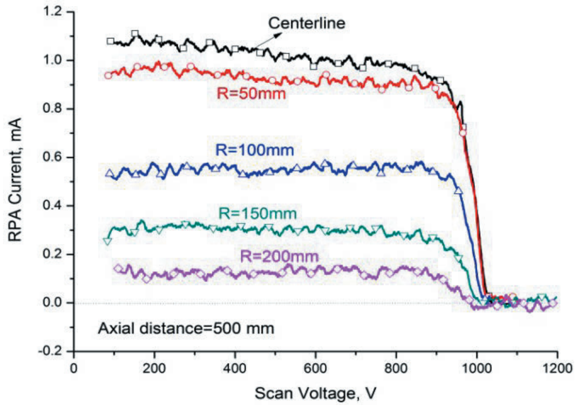

Figure 4. Radial RPA I-V curves.

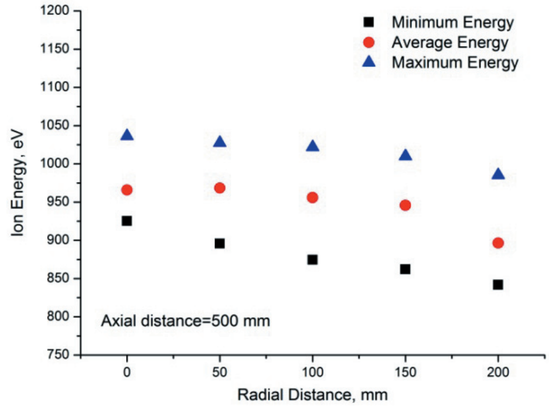

Figure 5. Radial ion energy distributions.

RPA axial scan measurements were performed from an axial position of 400 mm to 900 mm from the grid surface of the thruster. Because there is an obvious space charging effects when measurements were performed at 400 mm downstream, we could not take it any nearer to the thruster. RPA I-V curves at different axial locations are presented in Fig. 6. And the axial ion energy distribution is plotted in Fig. 7, from which it can be seen that the ion energy remains nearly constant as the increased axial distances.

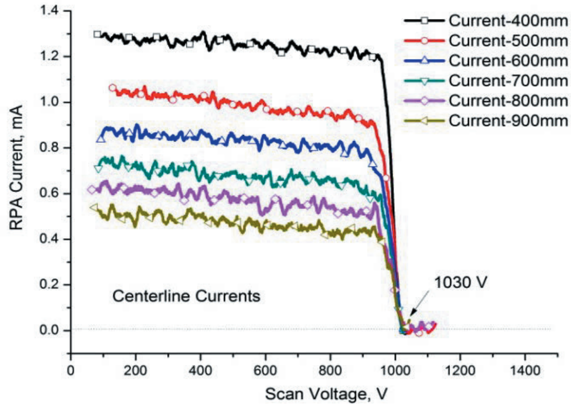

Figure 6. Axial RPA I-V curves.

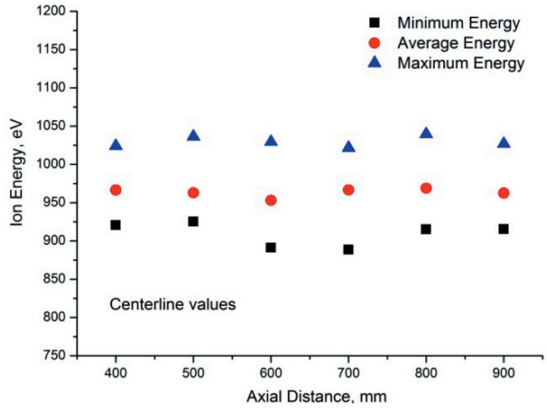

Figure 7. Axial ion energy distributions.

B. Faraday probe

Faraday probe measurements were performed from an axial position of 250 mm to 900 mm from the grid surface of the thruster and a radial position from the centerline to 400 mm off centerline. A 1000 Ohm shunt resistance was used to record the loop current. The current density was calculated by Eq. (1) at a specific location, and then all the values were plotted in a 2-D contour map, as shown in Fig. 8. From the contour map we can see that the current density researches its maximum at the centerline near the thruster and decrease with both the increased radial and axial distances. Also, larger current density gradient is along the radial direction.

We have examined the centerline current density distribution along the axial positions, as shown in Fig. 9. The black square is the experimental results and the red solid line is a cubic fit of the experimental data. And the blue triangle is the $1/z^2$ fit using the 250 mm experimental value as the reference data. From this figure we can see that the $1/z^2$ fit could not give the accurate current density prediction along axial directions, whereas the cubit fit agrees well with the experimental results. Four parameters in the cubic fit are also shown in Fig. 9, and the parameter A could indicate the current density value at the exit plane of the thruster.

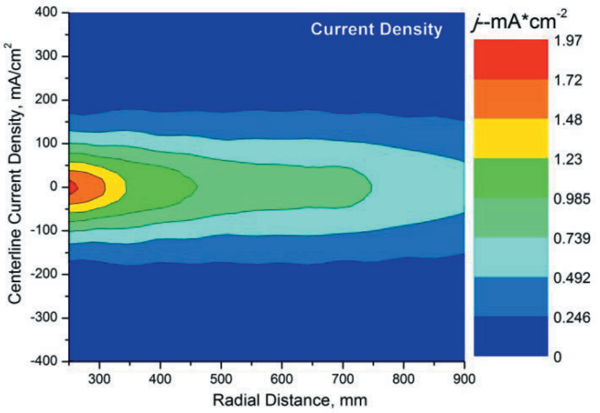

Figure 8. Current density contour map from Faraday probe.

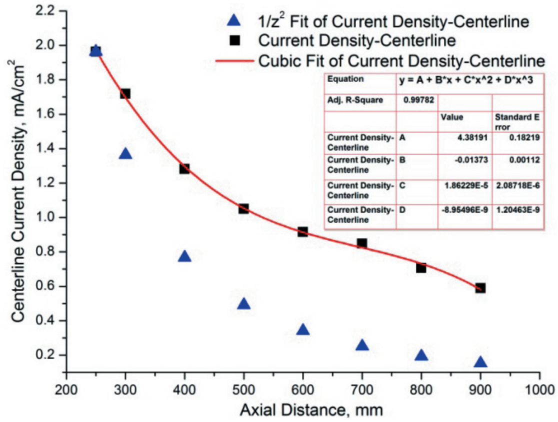

Figure 9. Centerline current density distributions.

C. Emissive probe

The heating current of the emissive probe has a huge influence on the hot probe's I-V characteristics. So we first provided several different heating currents to the emissive probe to identify the effect of these different currents on the probe's I-V curves, as shown in Fig. 10. When the heating currents are not very high such as 1-2.2 A, the electron emission is not obvious, whereas when the heating currents increase up to 2.3-2.5 A, the electron emission is obvious showing a sharp increase in collected electron currents. We can see that the I-V curves with different heating currents overlapped on a cross point, which is determined to be the plasma potential.

There are several techniques to determine the plasma potential from emissive probe I-V characteristics, such as the separation point, cross point, inflection point, floating potential inference, inflection point in the limit of zero emission methods and so on. Here we have considered the separation point, cross point, inflection point methods to determine the plasma potential from a same I-V curve, as shown in Fig. 11. As for the inflection point method, we referred to the voltage where the first order derivative I-V curve reaches its maximum and the second order derivative I-V curve is zero. The plasma potential determined from the separation point method is 22.96 V and that from the cross point is 18.59 V. These two methods agree with each other very well. The plasma potentials determined from the inflection point method including the first and second order derivative of the I-V curve are much smaller than the former two methods. Other techniques to determine the plasma potential from emissive I-V characteristics are still in investigations.

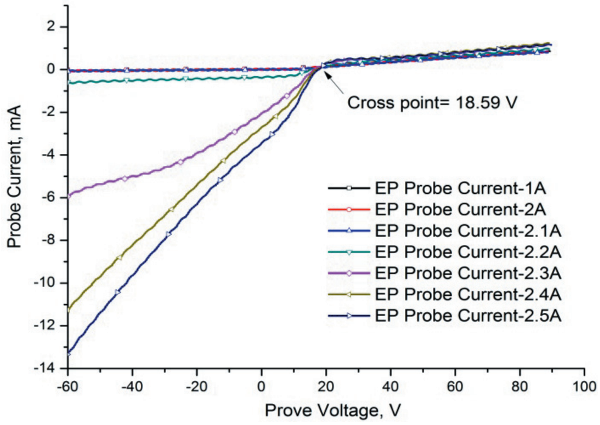

Figure 10. Emissive probe I-V curves with different currents.

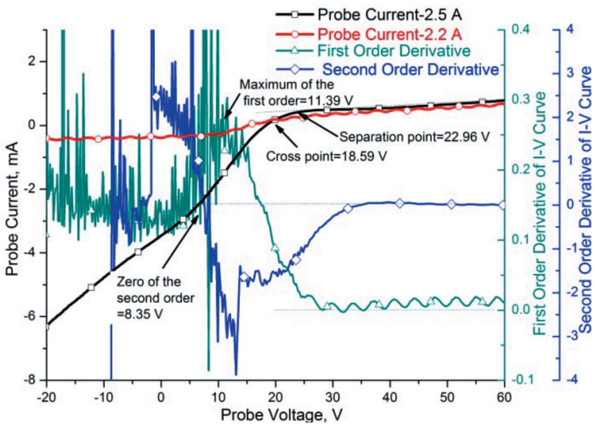

Figure 11. Determination of plasma potential.

D. Triple Langmuir probe

The measured voltage difference V_{d2} between the positive and floating wires, at a position of 300 mm downstream on the centerline of the thruster, is shown in Fig. 12. There is a regular oscillation with a magnitude of ±0.3 V comes along with the voltage signal. Since the frequency of the scan voltage for RPA is about 0.3 Hz and that for single Langmuir probe is 1 Hz, the regular 1 Hz noise must results from the voltage scan for the single Langmuir probe, which indicates the influence of other probes on the specific probe. Then, a linear fit to the voltage difference was performed to reduce the effect of the noise on the voltage and therefore the electron temperature. The measurement of the loop current I_3 is shown in Fig. 13, which is not largely influenced by the 1 Hz noise. Also, the linear fit was performed to get an accurate current value.

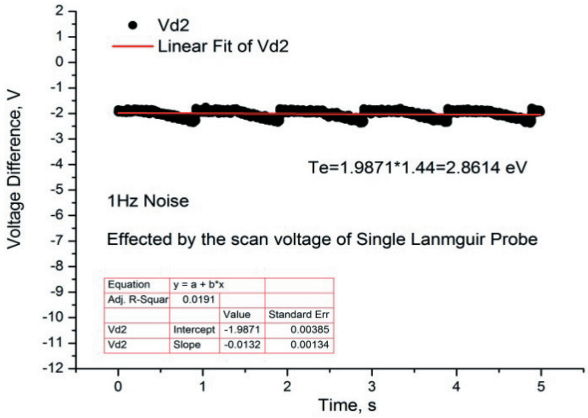

Figure 12. Measurement of the voltage difference V_{d2}.

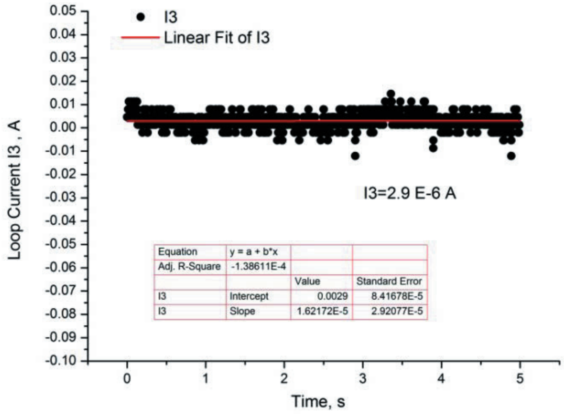

Figure 13. Measurement of the loop current I_3.

Since the values of V_{d2} and I_3 are known, the electron temperature and density could be derived by the Eqs. (2) and (3) respectively. The calculated electron temperature and density profiles as function of radius at the 300 mm and 500 mm axial positions are shown in Figs. 14 and 15, respectively. We can see that the electron temperature at 300 mm is higher than that at 500 mm at the same radial position within a radius of 150 mm, but reversed beyond this radius. At both axial locations, the electron temperature decrease with increased radius. The electron density at nearer axial position is higher and it also decreases with increased radius.

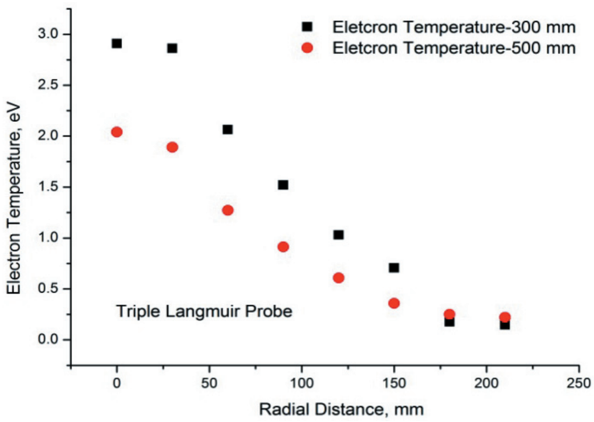

Figure 14. Radial electron temperature distribution.

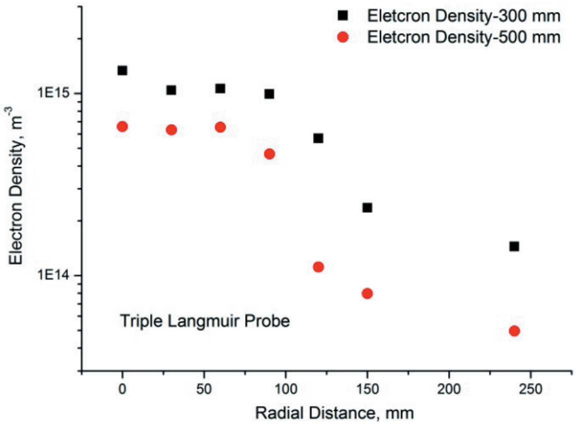

Figure 15. Radial electron density distribution.

E. Single Langmuir probe

Figure 16 shows the original and smoothed single Langmuir probe I-V curves at the location of 300 mm downstream on the centerline of the thruster. The Savitzky-Golay smoothing method imbedded in the Origin Pro 8 software is used here, which is also described in detail as shown in Fig. 16. From the smoothed I-V curve, the floating potential V_f was first determined by finding the voltage where the net current was zero, as shown in Fig. 17. The ion saturation current I_{sat} can be extrapolated back to V_f to obtain a better value before the expansion of the sheath, as also shown in Fig. 17. Then the probe current is plotted semi-logarithmically versus the probe voltage V_p. The electron temperature was calculated as the inverse slope of the $ln(I)$-V curve as shown in Fig. 18. The plasma potential was determined by the cross point of the linear fits of the transition and electron saturation regions, as shown in Fig. 19.

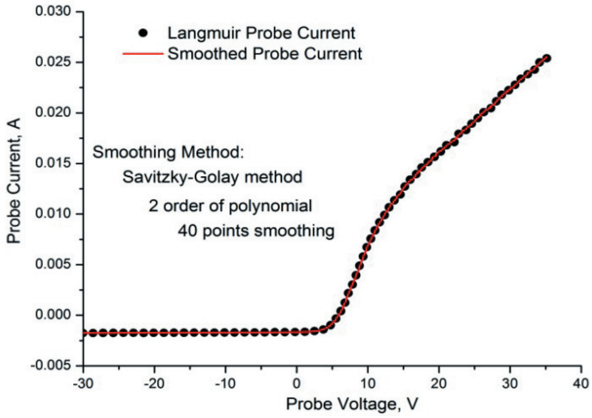

Figure 16. Original and smoothed I-V curve.

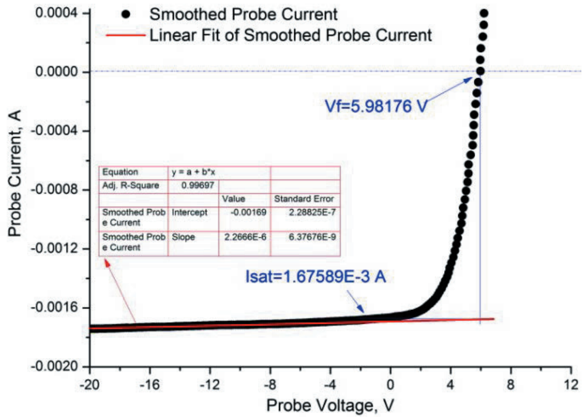

Figure 17. Determination of V_f and I_{sat}.

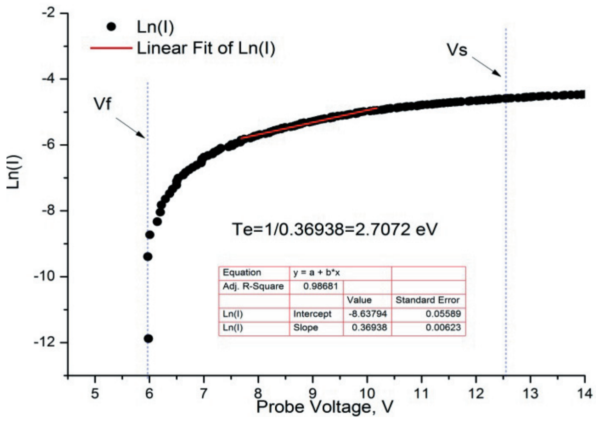

Figure 18. Determination of electron temperature.

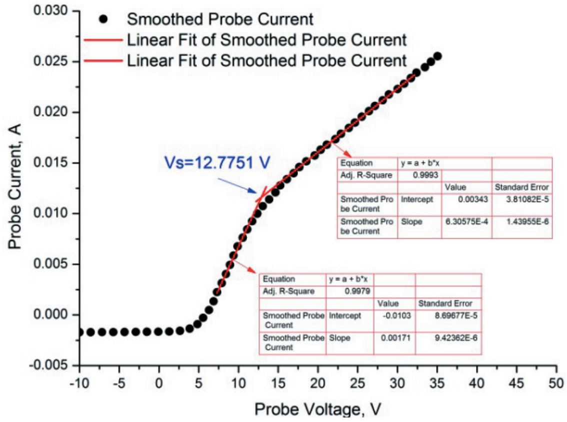

Figure 19. Determination of plasma potential.

The calculated electron temperature and density profiles along radius at the 300 mm and 500 mm axial positions are shown in Figs. 20 and 21, respectively. The general trends of the electron temperature and density as a function of radial and axial distances derived from the single Langmuir probe method are identical with that from triple Langmuir probe method as described above. However, the electron temperature derived from the single Langmuir probe is about 1 eV higher than that from triple Langmuir probe method. The reason is still under investigation. The electron density profiles derived from these two methods agree well with each other.

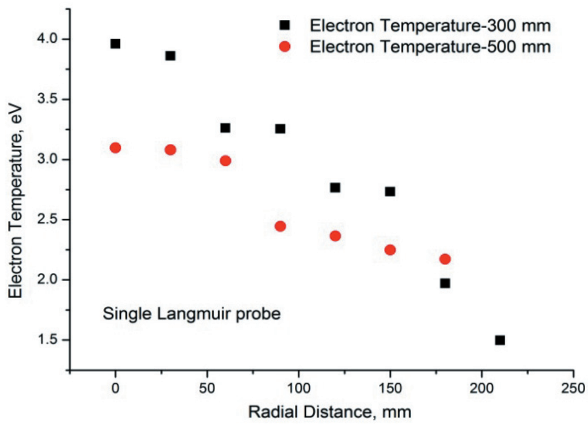

Figure 20. Radial electron temperature distribution.

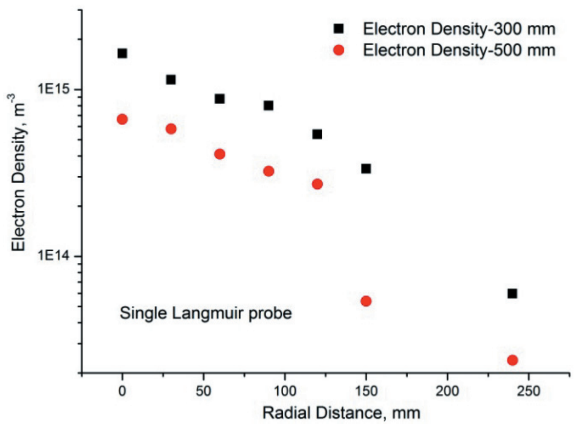

Figure 21. Radial electron density distribution.

IV. Conclusion

The plume plasma properties of a laboratory model ion thruster have been investigated thoroughly by a multiple-probe array. The ion energy distributions along radial and axial directions were identified by a three grids RPA. The results show that the ion energy decreases a little with the increased radius whereas the centerline ion energy remains constant with the increased axial distances.

The Faraday probe has been used to plot the current density contour map, which shows a maximum current density at the centerline near the thruster and a decreased value with both the increased radial and axial distances. Moreover, a cubic fit of the experimental centerline current density along axial distances could give more accurate prediction of the current density values than the $1/z^2$ fit.

The emissive probe has been applied to accurately determine the plasma potential, which could be of significant different values by different emissive probe techniques. The plasma potential determined by the separation point and cross point methods agree well with each other.

Electron temperature and density profiles have been calculated from both the single and triple Langmuir probe. The electron density profiles derived from these two methods match well with each other. However, the electron temperature derived from the single Langmuir probe is about 1 eV higher than that from the triple Langmuir probe, which is still under investigation.

Acknowledgments

This work was supported by the National Natural Science Foundation of China (No. 51276006)

References

[1]De Boer, P. C. T., ‘‘Measurements of Electron Density in the Charge Exchange Plasma of an Ion Thruster,’’ *Journal of Propulsion and Power*, Vol. 13, No. 6, 1997, pp. 783-788.

[2]Rovey, J. L., and Gallimore, A. D., “Dormant Cathode Erosion in a Multiple-Cathode Gridded Ion Thruster,” *Journal of Propulsion and Power*, Vol. 24, No. 6, 2008, pp. 1361-1368.

[3]Wang, J., Brinza, D. E., Young, D. T., etc., “Deep Space One Investigations of Ion Propulsion Plasma Environment,” *Journal of Propulsion and Power*, Vol. 37, No. 5, 2000, pp.545-555.

[4]Milligan, D. J., and Gabriel, S. B., “Investigation of the Baffle Annulus Region of the UK25 Ion Thruster,” *AIAA* 99-2440.

[5]T. Zhang, et al., “Initial Flight Tests Results of the LIPS-200 Electric Propulsion System on SJ-9A Satellite”, *IEPC*-2013-47.

[6]Monterdey, M. P., Hainesy, M. G., Dangory, A. E., Maliky, A. K., and Fearnz, D. G., “Kaufman-type xenon ion thruster coupling plasma: Langmuir probe measurements,” *Journal of Physics D-Applied Physics*, No. 30, 1997, pp.842–855.

[7]Milligan, D. J., and Gabriel, S. B., “Investigation of the Baffle Annulus Region of the UK25 Ion Thruster,” *AIAA* 99-2440.

[8]M. R. Carruth, “A Review of Studies on Ion Thruster Beam and Charge-Exchange Plasmas”, *AIAA*1982-1944.

[9]J. M. Jr. Sellen, W. Bernstein, and R. F. Kemp, “Generation and Diagnosis of Synthesized Plasma Streams”, *Review of Scientific Instruments*, Vol. 36, No. 316, 1965.

[10]Allan J. Coben, “Anomalous Diffusion in a Plasma Formed from the Exhaust Beam of an Electron-Bombardment Ion Thruster”, *NASA TN* D-4758, August 1968.

[11]G. K. Komatsu, et al, “Charge Exchange Ion Formation and Motion in Mercury Ion Engine Thrust Beams”, *AIAA* 75-428.

[12]G. K. Komatsu and J. M. Sellen, “Beam Efflux Measurements for a 38 cm Mercury Ion Thruster”, *AIAA* 76-1052.

[13]P. C. T.De Boer, “Electric Probe Measurements in the Plume of an Ion Thruster”, *Journal of Propulsion and Power*, Vol. 12, No. 10, 1996, pp. 95-104.

[14]Dennis Keefer, and V. V. Semak, “Measurements of radial and axial distributions of ion thruster plasma parameters using a Langmuir probe”, *AIAA* 96-2984.

[15]J.Wang, et al, “Deep Space One Investigations of Ion Propulsion Plasma Environment”, *Journal of Spacecraft and Rockets*, Vol. 37, No. 5, 2000, pp. 545-555.

[16]T.Ozaki, et al., “Development Status of 20 mN Class Xenon Ion Thruster for ETS-8”, *IEPC* 2001-102.

[17]N.Yamamoto, et al., “Measurement of Plasma Property in an Ion Thruster using Laser Thomson Scattering Technique”, *IEPC* 2011-200.

[18]Y. Wang, et al., “Life Tests and Measurements of Ion Thruster Accelerator Grid Erosion”, *AIAA* 2008-4528.

[19]T. Zhang, et al., “Initial Flight Tests Results of the LIPS-200 Electric Propulsion System on SJ-9A Satellite”, *IEPC*-2013-47.

[20]C. K. Chao and S.-Y. Su, “Charged particle motion inside the retarding potential analyzer”, *Physics of Plasmas*, Vol. 7, No. 101, 2000.

[21]Brian E. Beal and Alec D. Gallimore, “Energy Analysis of a Hall Thruster Cluster”, *IEPC*-2003-35.

[22]Zun Zhang, Haibin Tang, Mengdi Kong, Zhe Zhang, and Junxue Ren, “Electron temperature measurement in Maxwellian non-isothermal beam plasma of an ion thruster,” *Review of Scientific Instruments,* Vol. 86, No. 023506, 2015.

[23]Yassir Azziz and Manuel Martinez-Sanchez, "Experimental and Theoretical Characterization of a Hall Thruster Plume", Ph.D. Dissertation, Department of Aeronautics and Astronautics, Massachusetts Institute of Technology, Cambridge, MA, 2007.
[24]Shastry, R., and Gallimore, A. D., "Near-Wall Plasma Properties and EEDF Measurements of a6-kW Hall Thruster," *AIAA* 2009-5356.
[25]J. P. Sheehan, Y. Raitses, N. Hershkowitz, I. Kaganovich, and N. J. Fisch, "A comparison of emissive probe techniques for electric potential measurements in a complex plasma," *Physics of Plasmas*, Vol. 18, No. 073501, 2011.
[26]Chen, S. L., and Sekiguchi, T., "Instantaneous Direct-Display System of Plasma Parameters by Means of Triple Probe," *Journal of Applied Physics*, Vol. 26, No. 8, 1965, pp. 2363–2375.
[27]Eckman R. F., "Langmuir Probe Measurements in the Plume of a Pulsed Plasma Thruster," Science Master Degree Dissertation, Mechanical Engineering, Worcester polytechnic institute, MA, 1999.
[28]S. G. Lee and J. G. Bak, "Triple Langmuir probe measurements in the Hanbit magnetic mirror device", *Review of Scientific Instruments*, Vol. 72, No. 442, 2001.
[29]Chen, F. F., "Lecture Notes on Langmuir Probe Diagnostics," *IEEE-ICOPS* Meeting, Jeju, Korea, June 5, 2003.
[30]Daniel Andrew Herman, "The Use of Electrostatic Probes to Characterize the Discharge Plasma Structure and Identify Discharge Cathode Erosion Mechanisms in Ring-Cusp Ion Thrusters", Ph.D. Dissertation, Aerospace Engineering, The University of Michigan, MI, 2005.
[31]Daniel A. Herman, and Alec D. Gallimore, "A High-Speed Probe Positioning System for Interrogating the Discharge Plasma of a 30 cm Ion Thruster" *AIAA*-2002-4256.